Tubby-like protein 4 negatively regulates hedgehog signaling in osteoblast lineage cells

Sung-Jin Kim

The Graduate School

Yonsei University

Department of Dentistry

Tubby-like protein 4 negatively regulates hedgehog signaling in osteoblast lineage cells

Directed by Professor Hyoung-Seon Baik

The Doctoral Dissertation Submitted to
the Department of Dentistry,
the Graduate School of Yonsei University
in partial fulfillment of the requirements
for the degree of Ph.D. in Dental Science

Sung-Jin Kim

June 2016

연세대학교
YONSEI UNIVERSITY

This certifies that the Doctoral Dissertation

of Sung-Jin Kim is approved.

Thesis supervisor: Hyoung-Seon Baik

Kee-Joon Lee

Chooryung Chung

Seok Jun Moon

Chul Hoon Kim

The Graduate School

Yonsei University

June 2016

ACKNOWLEDGEMENTS

부족한 저를 항상 아낌없는 가르침과 격려로 이끌어주시고 보살펴 주시는 백형선 교수님께 진심으로 감사 드립니다. 그리고 기초학에 대한 지식도 경험도 전무한 저를 받아주시고 논문이 나오기까지 세심하게 지도해 주신 문석준 교수님께 깊이 감사 드립니다. 바쁘신 와중에도 많은 관심과 조언으로 부족한 논문을 살펴주신 이기준 교수님, 정주령 교수님, 김철훈 교수님께 감사 드리고, 교정의로 거듭날 수 있도록 따뜻한 말씀과 가르침으로 보살펴 주신 박영철 교수님, 황충주 교수님, 김경호 교수님,유형석 교수님,차정열 교수님,최윤정 교수님께 감사 드립니다.또한 항상 따뜻한 말씀으로 격려와 가르침을 주시는 서정택 교수님과 신동민 교수님께 감사 드립니다.

약리학 교실에서 생활하면서 많은 도움을 주신 박지나 선생님, 정용택 선생님, 정경화 선생님, 유윤정 선생님께 감사 드리고, 특히 수많은 질문에도 귀찮은 내색 없이 친절하게 실험을 가르쳐 주시는 오수영 선생님께 감사 드립니다. 그리고 기쁘고 힘든 시간들을 함께한 약리학 교실 동료 박용욱, 이나영, 박소영, 오수민 선생과 생리학 교실 이소윤, 선지수, 김슬기, 강남주, 박순홍 선생에게도 이 자리를 빌려 감사의 마음을 전합니다.

마지막으로 늘 곁에서 힘이 되어주는 사랑하는 아내 선영이와 항상 변함없는 사랑과 응원을 보내주시는 부모님과 동생에게 고마움을 전합니다.

CONTENTS

List of Figures

List of Tables

ABSTRACT

Tubby-like protein 4 negatively regulates hedgehog signaling in osteoblast lineage cells

Sung-Jin Kim

Department of Dentistry
The Graduate School, Yonsei University
(Directed by Professor Hyoung-Seon Baik)

Tubby-like protein 4 (*Tulp4*) is a member of Tubby superfamily. Although several previous studies have suggested a possibility that *Tulp4* might be related to bone homeostasis, no function of *Tulp4* has been reported yet. Therefore, the purpose of this study was to investigate possible roles of *Tulp4* in bone homeostasis.

In this study, osteoblast-specific *Tulp4* knockout mice were generated using Cre-lox system to investigate the function of *Tulp4* in bone formation *in vivo*. Also, osteoblastic differentiation was investigated by *in vitro* culture of primary mouse calvarial osteoblasts.

Tulp4 was expressed in bone, and its expression was increased during early phase of osteoblastic differentiation. Although *Tulp4* global knockout mice showed neonatal lethality with no bone phenotype, osteoblast-specific *Tulp4* knockout adult mice showed osteopetrotic phenotype, indicating that *Tulp4* negatively regulates bone homeostasis. Osteoblastic differentiation was enhanced in *Tulp4* knockout primary osteoblasts, suggesting *Tulp4* inhibits osteoblastic differentiation in a cell-autonomous manner. In *Tulp4* knockout primary osteoblasts, hedgehog signaling was enhanced, which was demonstrated by increased mRNA levels of *Patched1* and *Gli1*. This enhanced hedgehog signaling was due to the increased expression of *Ihh*, and 5E1 hedgehog neutralizing antibody blocked the hedgehog phenotype. Western blot analysis of subcellular fractionation and immunofluorescent staining showed that TULP4 was localized to nucleus in primary osteoblasts.

In summary, this study demonstrated novel functions of *Tulp4* that inhibit bone formation and negatively regulate hedgehog signaling by inhibition of *Ihh* expression.

Key words: Tubby-like protein 4, bone, osteoblastic differentiation, hedgehog

Tubby-like protein 4 negatively regulates hedgehog signaling in osteoblast lineage cells

Sung-Jin Kim

Department of Dentistry

The Graduate School, Yonsei University

(Directed by Professor Hyoung-Seon Baik)

Ⅰ. INTRODUCTION

Bone is a dynamic vascular mineralized connective tissue. Its homeostasis is maintained by the balance between the bone-forming osteoblasts and the bone-resorbing osteoclasts. Osteoblasts and osteoclast have different origins: while osteoblasts originate from multipotent mesenchymal stem cells, osteoclasts originate from granulocyte-macrophage progenitors of the hematopoietic origin.

However, two types of cells are closely coupled to each other for physiological bone remodeling. For example, osteoblasts secrete molecules that can bind to osteoclasts and control its differentiation, such as RANKL and M-CSF, while osteoclastic bone resorption releases some cytokines that recruit and stimulate osteoblast differentiation. Imbalance of the coupling process can lead to debilitating bone diseases, including osteoporosis, osteopetrosis, and periodontitis (Phan et al., 2004).

Osteoporosis is a systemic skeletal disorder with low bone mass caused by imbalance of osteoblasts and osteoclasts activities favoring osteoclastic bone resorption. It is characterized by high susceptibility to fractures, such that half of Caucasian women and a fifth of men are expected to experience bone fracture due to osteoporosis in the course of lifetime (Cosman et al., 2014). It also causes enormous socioeconomic burden for treatment of osteoporosis-related fracture, costing nearly $17 billion in 2005 in the United States, and predicted to be doubled or tripled within the next four decades due to rapid aging of populations (Burge et al., 2007).

Therapies for osteoporosis can be divided into two categories: anabolic therapeutic for increasing osteoblastic bone formation and anti-

catabolic therapeutic for inhibiting osteoclastic bone resorption. Currently, the only anabolic therapeutic approved by the Food and Drug Administration is parathyroid hormone (PTH). Intermittent administration of PTH results in an increase in bone mass, but long term administration is limited due to the report that almost half of the rats treated with PTH at high dose developed osteosarcoma (Vahle et al., 2002). There are several anti-catabolic therapeutics in use, such as bisphosphonate, but those drugs are associated with some side effects including bowel inflammation and bisphosphonate-related osteonecrosis of the jaw (Kumar and Sinha, 2014). Moreover, these anti-catabolic agents cannot be used in bone fracture healing. In this regard, studies of osteoblastic differentiation have clinical significance for development of anabolic therapeutics that safely and effectively stimulate osteoblast formation and activity.

Tubby-like protein 4 (*Tulp4*) is a member of Tubby superfamily that is characterized by C-terminal conserved Tubby domain. The function of Tubby domain is still not fully understood, although it can bind to biphosphorylated phosphoinsitides and DNA (Ikeda et al., 2002; Mukhopadhyay et al., 2010). TULPs have indispensable role in neuronal development, such that *Tulp3* knockout mice, for example, showed

embryonic lethality with neural tube defects and neuroepithelial cell death (Ikeda et al., 2001). Also, *Tulp3* is known to be a negative regulator of hedgehog signaling via ciliary trafficking of GPR161(Mukhopadhyay et al., 2013).

Tulp4, located to mouse chromosome 17q13, was first cloned and characterized by Li et al.(Li et al., 2001) in 2001. TULP4 protein sequences are less identical (40~48%) in the C-terminal region to other tubby family proteins, which showed 55~90% identity, indicating it is a distant relative of the family member. TULP4 has several functional domains, including a tubby signature motif (FxGRVTQ), one WD40 repeat region and one suppressor of cytokines signaling (SOCS) domain (Li et al., 2001). However, no function of *Tulp4* has been reported yet.

Several previous studies suggest a possible role of *TULP4* in bone homeostasis. Single nucleotide polymorphism (SNP) in 3'UTR of *TULP4*, which may affect the expression level of TULP4, was associated with short stature in human by genome-wide association study (Lango Allen et al., 2010). Also, genetic variants in *TULP4* gene was associated with cleft lip with or without cleft palate (Vieira et al., 2015). Mutations in *WDR35*, a homolog of *TULP4*, were responsible for Sensenbrenner syndrome, which

shows bone phenotype, such as sagittal suture synostosis, metaphyseal dysplasia, and dwarfism (Lin et al., 2013).

The purpose of this study was to investigate possible roles of *Tulp4* in bone homeostasis. We generated osteoblast-specific *Tulp4* knockout mice, and osteoblastic differentiation was also investigated *in vitro* by using primary mouse calvarial osteoblasts. We demonstrated that *Tulp4* inhibits bone formation and negatively regulates hedgehog signaling by inhibition of *Ihh* expression.

Ⅱ. MATERIALS AND METHODS

1. Animal experiments

Mouse embryonic stem cells containing a null mutation in *Tulp4* gene (*Tulp4*$^{tm1a(KOMP)Wtsi}$) were purchased from the Knockout Mouse Project (KOMP). Mice containing a *Tulp4*^{tm1a} allele(*Tulp4*(+/1a)) with C57BL/6N background were generated by Macrogen (South Korea). *Tulp4*(+/1a) mice were crossed with transgenic Rosa-Flipase(FLP) mice (129S4/SvJae-Gt(ROSA) 26Sor$^{tm2(FLP*)Sor}$/J), purchased from Jackon Laboratory, to generate FLP+;*Tulp4*(+/1c), and FLP allele was removed by crossing with wild-type mice. *Tulp4* global knockout mice (hereafter called *Tulp4*(-/-)) were generated by crossing *Tulp4*(1c/1c) mice with transgenic CMV-Cre mice. Osteoblast-specific *Tulp4* knockout mice were generated by crossing *Tulp4*(1c/1c) mice with osteocalcin-Cre mice (B6N.FVB-Tg(BGLAP-cre)1Clem/J) purchased from Jackon Laboratory. General mating scheme of knockout first allele and that of osteoblast-specific *Tulp4* knockout mouse in this study are presented in Figure 1. All wild-type mice were purchased from Central Lab. Animal Inc. on a C57BL6/J background.

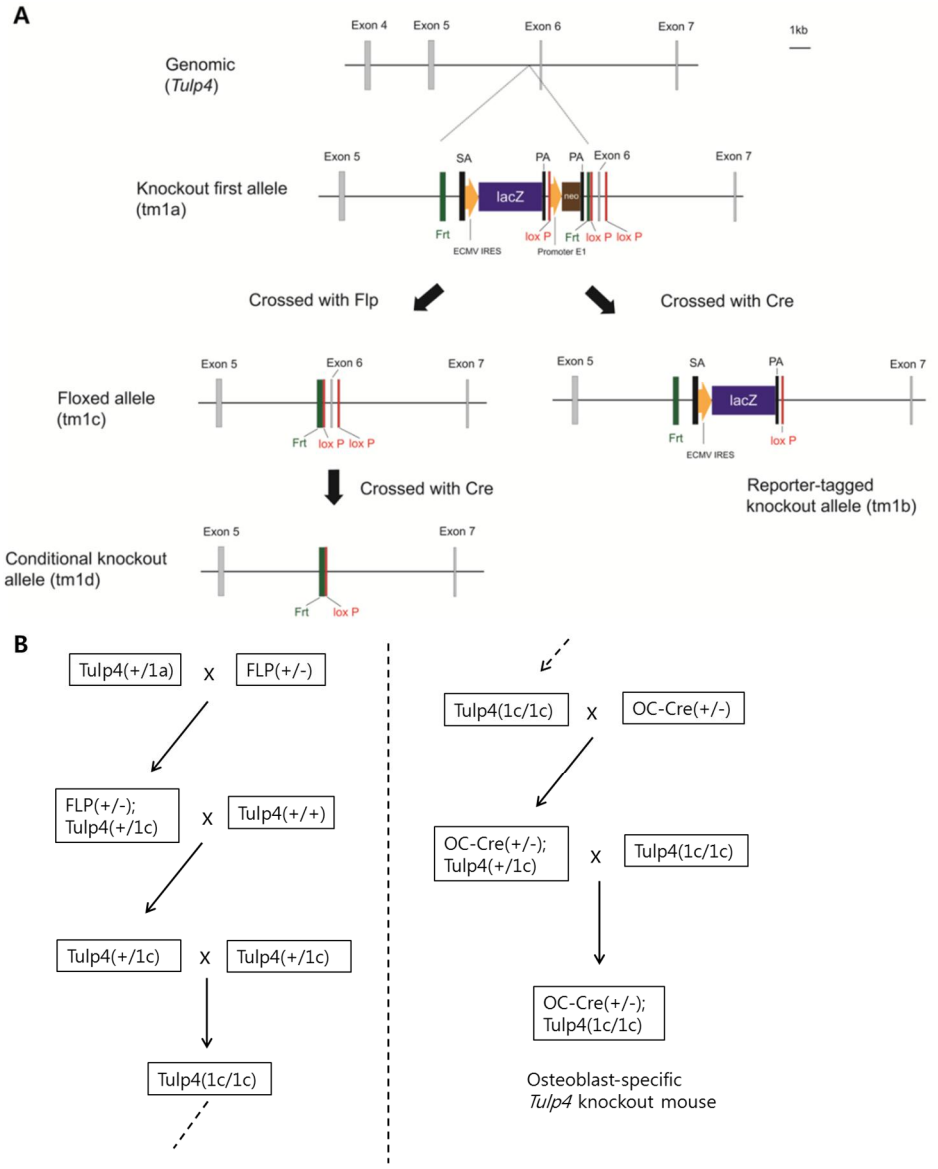

Figure 1. A. General mating scheme of knockout first allele. B. Mating scheme of osteoblast-specific *Tulp4* knockout mouse using transgenic osteocalcin-Cre mice in this study

Mice were housed 3-5 per cage in a temperature- and humidity-controlled environment (lights on 08:00-20:00). Food and water were available *ad libitum*. All animal experiments were approved by the Animal Care Committee of Yonsei University College of Medicine.

2. Genomic DNA preparation and genomic PCR

For DNA isolation from the mouse tail, 0.5mm of mouse tail was removed into EP tube and digested with MyTaq™ Extract-PCR kit (Bioline, UK) according to the manufacturer's recommended protocol. Briefly, 10μl of Buffer A, 5μl of Buffer B, and 35μl of distilled water (Water, Ultra pure, Biosolution) were added into a tube containing a tail, and digested at 75℃ for 10 minutes, followed by 95℃ for 10 minutes.

The PCR reactions were performed using MyTaq™ Extract-PCR kit in Veriti 96-well thermal cycler (Applied Biosystems, US). The reaction mixture for one 20μl reaction contained 10μl MyTaq HS Red Mix, 1μl forward and reverse primers (final concentration of 500nM), 7μl Ultra pure water, and 1μl template DNA. The reaction mixture was transferred

into 0.2ml PCR tube, and incubated for 5 minutes at 94℃ and then 40 cycles of PCR reaction were run at 94℃ for 15 seconds, 55℃ for 30 seconds, and 72℃ for 40 seconds, followed by incubation for 5 minutes at 72℃. The annealing temperature were initially started at 65℃ and then decreased 1℃ per one cycle until it reached at 55℃. The genotyping scheme and primers are presented in Figure 2 and Table 1.

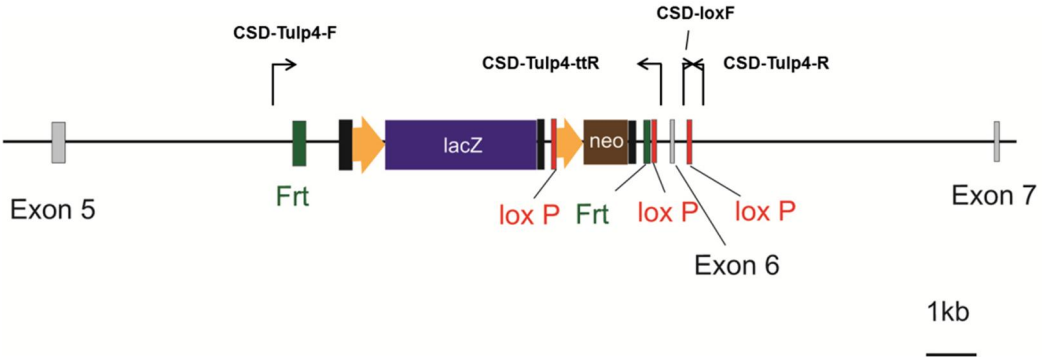

Figure 2. Location of primers used for genotyping

Genotype	Forward primer	Reverse primer	Amplicon size (bp)
Wild-type	CSD-Tulp4-F	CSD-Tulp4-ttR	466
Tulp4 tm1a	CSD-loxF	CSD-Tulp4-R	351
Tulp4 tm1c	CSD-Tulp4-F	CSD-Tulp4-ttR	620
Tulp4 tm1d	CSD-Tulp4-F	CSD-Tulp4-R	720

Primer	Sequence (5'→3')
CSD-Tulp4-F	GATTTCTCCACTCATGCTACCTGGC
CSD-Tulp4-ttR	AAGGCAAAAGGGTCACAGTTAAGGC
CSD-lox-F	GAGATGGCGCAACGCAATTAATG
CSD-Tulp4-R	TCTGGGACTTCCATTTGTCTCCACC
Cre-F	TCCAATTTACTGACCGTACACCAA
Cre-R	CCTGATCCTGGCAATTTCGGCTA

Table 1. Primers used for genotyping

3. Bone and cartilage staining in neonatal pups

Mouse neonates were submerged into ice for 20 minutes and scalded in hot tap water (65~70℃) for 20~30 seconds. The skin was carefully peeled off with forceps and the neonates were eviscerated, including the contents of the peritoneal and pleural cavities. Neonates were fixed in 95% ethanol overnight, and then transferred to acetone at room temperature overnight to remove fat. Neonates were rinsed briefly in deionized water and placed in alcian blue staining solution (Alcian blue 8GX (Sigma Cat# A5268, 0.03% (w/v) in 80% ethanol and 20% acetic acid)) for 24 hours to stain cartilage. Neonates were washed in 70% ethanol for 6~8 hours, and then placed in 1% potassium hydroxide solution (KOH) until the tissues are visibly cleared. Neonates were placed in alizarin red staining solution (Sigma Cat#A5533, 0.05% in 1% (w/v) KOH) overnight to counterstain bone, and cleared by placing them in 1% KOH/20% glycerol for 2 days. The samples were stored in a 1:1 mixture of glycerol and ethanol until imaging.

4. Micro-computed tomography(μCT) scanning and morphometric analysis

Femurs were removed from 17-week-old male littermates of Tulp4(1c/1c) and OC-Cre+;Tulp4(1c/1c), fixed in the 10% neutral buffered formalin for 2 days at room temperature, and then stored in 70% ethanol at 4℃ until μCT scanning.

Femurs were scanned by SkyScan 1173 (Bruker, Belgium) with isotropic voxel size of 7.10 μm, using settings of 90kV, 88μA, a 1.0mm aluminium filter, and X-ray detector with 2240 x 2240 pixels. The acquired images were reconstructed into cross section images by NRecon (version 1.6.10, Bruker, Belgium), and then analysed in CTAn (version 1.16, Bruker, Belgium). A region of interest (ROI) was defined as 0.5~1.7mm above the distal growth plate of the femur and a grayscale threshold value range of 62~255 was used for morphometric analysis. Trabecular bone volume fraction, trabecular number, thickness, and separation were calculated. Three-dimensional volume-rendered images were acquired using CTVox (version 3.1.2, Bruker, Belgium).

5. Histological and morphometric analysis

Following μCT scanning, the femurs were decalcified using ChelatorCal™ (BBC biochemical, US) for 2 weeks at room temperature. After decalcification, the specimens were processed for paraffin embedding, of which 4 μm longitudinal sections were obtained and stained with hematoxylin and eosin (H&E). The whole slide was digitally scanned using Panoramic 250 Flash III (3D histech, Hungary).

For histomorphometric analysis, osteoblast-like cells on bone surfaces were counted and divided by the total length of bone surface in a region of interest measured using ImageJ (version 1.49, NIH, US).

6. Primary mouse calvarial cell culture

The neonates (P0) from *Tulp4* (1c/-)(= *Tulp4* (1c/△)) x *Tulp4* (1c/-) mating pair were removed and tails were cut for genotyping. After the results of genotyping were confirmed, *Tulp4* (1c/1c) (wild-type) and *Tulp4* (-/-) neonates were used for subsequent primary calvarial cell culture.

Neonates were euthanized by immersing them in 70% ethanol. The calvaria were removed and collected in serum free α-MEM (Gibco, US), and transferred to 50ml tube containing 10ml 0.2μm-filtered enzyme solution (α-MEM + 0.2% Dispase (Gibco, US) + 0.1% Collagenase type IV (Sigma-Aldrich, US) + 1% penicillin/streptomycin). The calvaria were incubated for 10 minutes at 37℃ with shaking, and supernatant was discarded. Again, 10ml enzyme solution was added to the tube containing calvaria, incubated for 20 minutes at 37℃ with shaking, and supernatant was collected in a new 50ml tube. This step was repeated 3 times. Collected 30ml supernatant was filtered using 70μm Cell Strainer (Falcon, US), and centrifuged at 300xG for 3 minutes. The cells were resuspended in complete growth medium (α-MEM + 10% fetal bovine serum (FBS, Gibco, US) + 1% penicillin/streptomycin), and split to one 100mm culture dish per one calvaria (approximately 2 x 10^6 cell/ 100mm dish).

The cells were cultured at 37℃ with an atmosphere of 5% CO_2 and 95% humidity, and the medium was changed every 2 or 3 days. When the confluency of cells reached to 80~90%, the cells were trypsinized and seeded to either 12 well (0.8 x 10^5 cell/well), 6 well (1.3 x 10^5 cell/well), or 60mm dish (2.9 x 10^5 cell/dish). Then, osteoblast differentiation was

induced by addition of 50μg/ml L-ascorbic acid and 10mM final concentration β-glycerol phosphate to the complete growth medium.

For blocking of hedgehog signalling, 5E1 antibody (obtained from hybridoma cells at the Developmental Studies Hybridoma Bank (DSHB)) or cyclopamine (Toronto Research Chemical, US) were added to the differentiation medium. For a control antibody, 40-1a (monoclonal antibody against β-galactosidase, obtained from hybridoma cells at the DSHB) was added.

7. Alkaline phosphatase staining

After 7 days of osteoblast differentiation in 12 well plates, culture medium was removed and washed with PBS 2 times, and fixed in 10% neutral buffered formalin for 1 minute. The cell layer was washed with deionized water (DW) 2 times, and 1ml BCIP®/NBT Liquid Substrate System was added to each well. The cells were incubated at room temperature for 10~20 minutes for color development, and washed with DW 2 times. The bottom of plate was photographed, and the quantification

was performed by averaging mean gray value using ImageJ (version 1.49, NIH, US).

8. Alizarin red S staining

To prepare the alizarin red staining solution, 0.136g alizarin red S (Alpha chem, UK) was dissolved in DW, and pH was adjusted to 4.1~4.3 with 0.5% NH_4OH, and the solution was filtered using 0.45μm Minisart syringe filter (Satorious, Germany).

After 21 days of osteoblast differentiation in 12 well plate, culture medium was removed and washed with PBS 2 times, and fixed in 10% neutral buffered formalin for 20 minutes at 4℃. The cells were washed with DW 2 times, and stained with 0.5ml alizarin red staining solution per each well in the dark at room temperature for 1 hour. Then, the solution was removed, and the cells were washed with DW until the DW became clear. The bottom of the plate was photographed.

For quantification of staining, 0.5ml 10% cetylpyridinium chloride (CPC) in DW was added to each well, and incubated at room temperature

with shaking for 1 hour. The CPC was collected in a 1.5ml EP tube. The cells were incubated with 0.5ml CPC again for 30 minutes and CPC was collected. This step was repeated one more time. The collected CPC was transferred to 96 well plate (0.2ml/well) in triplicate, and the absorbance was read at 570nm by using ELISA reader.

9. RNA extraction from cultured cell

Total RNA of cultured primary osteoblasts were isolated by using RNeasy Mini Kit (Qiagen, Germany) according to the manufacturer's protocol. The cell monolayer in 6 well plate was directly lysed with 350μl RLT buffer and transferred to 1.5ml RNase-free Eppendorf(EP) tube. The cell lysate was homogenized either by vortexing for 1 minute or using TissueLyser LT (Qiagen, Gernmany) with 3 ceramic beads for 1 minute. After homogenization, 350μl of 70% ethanol in DEPC-treated water was added and mixed by repetitive pipetting, and then transferred to the RNA-binding column and centrifuged for 30 seconds at 15000xG. The flow through was discarded and 700μl RW1 buffer was applied to the column and was centrifuged as previously. The flow through was discarded and

500μl RPE wash buffer was applied and centrifuged as previously. The flow through was discarded and 500μl RPE wash buffer was applied again and centrifuged for 2 minutes. Then, the column was transferred to a new 2ml collection tube and centrifuged for 1 minute to prevent the ethanol carryover. Finally, the column was transferred to a 1.5ml RNase-free EP tube and 30μl RNA-free water was applied and the column was centrifuged for 1 minute.

The purity and amount of the RNA was evaluated using NanoDrop system (Witec Gmbh, Germany) and 260/280 ratio and 260/230 ratio were calculated.

10. Real-time reverse transcriptase (RT)-PCR

Reverse transcriptase (RT) reaction was performed using RevertAid RT Kit (Thermo Fisher Scientific, US) according to the manufacturer's protocol. The calculated amount of RNA (2 or 3μg) was transferred in 0.2ml RNase-free tube, and 100pmol oligo$(dT)_{18}$ was added and DEPC-treated water was added upto 12.5μl. The sample was

incubated at 65℃ for 5 minutes using Veriti 96-well thermal cycler (Applied Biosystems, US) and placed on ice, and 4μl 5X reaction buffer, 0.5μl RiboLock (Thermo Fisher Scientific, US), 2μl dNTP mix, 10mM each, and 1μl RevertAid Reverse Transcriptase were added. The sample was then incubated for 60 minutes at 42℃. The RT reaction was terminated by heating at 70℃ for 10 minutes. The sample was then diluted by adding DEPC-treated water to make cDNA concentration of 50ng/3μl.

The real-time quantitative PCR(qPCR) reactions were performed in 96 well StepOnePlus (Applied Biosystems, US). The reaction mixture for one 20μl reaction contained 10μl SensiFAST SYBR Hi ROX mix (Bioline, UK), 1μl forward and reverse primers (final concentration of 500nM), 5μl Ultra pure water, and 3μl template cDNA (50ng). The reaction mixture was transferred into 0.2ml 8-strips (Axygen, US), incubated for 5 minutes at 95℃ and then 40 cycles of PCR reaction were run at 94℃ for 5 seconds, 60℃ for 10 seconds, and 72℃ for 15 seconds. The primers are presented in Table 2.

Target	Forward (5'→3')	Reverse (5'→3')
Tulp4	GACTTCGGAGGAAGGGTGAC	TAGGCGCTGAGTCACATTGG
Gapdh	AGGTCGGTGTGAACGGATTTG	TGTAGACCATGTAGTTGAGGTCA
Runx2	AGGGACTATGGCGTCAAACA	GGCTCACGTCGCTCATCTT
Sp7 (Osterix)	GTCCTCTCTGCTTGAGGAAGAA	GGCTGAAAGGTCAGCGTATG
Alpl	CCAACTCTTTTGTGCCAGAGA	GGCTACATTGGTGTTGAGCTTTT
Bglap (Osteocalcin)	CTGACAAAGCCTTCATGTCCAA	GCGCCGGAGTCTGTTCACTA
Col1a1	CTCCTGGTGAAGCAGGCAA	AACCTCTCTCGCCTCTTGCG
Ibsp (Bone sialoprotein)	ACAATCCGTGCCACTCACT	TTTCATCGAGAAAGCACAGGC
Spp1 (Osteopontin)	ACTCCAATCGTCCCTACAGTCG	TGAGGTCCTCATCTGTGGCAT
Ptch1	GCCTTCGCTGTGGGATTAAAG	CTTCTCCTATCTTCTGACGGGT
Gli1	TACCATGAGCCCTTCTTTAGGA	GCATCATTGAACCCCGAGTAG
Gli2	GCAGACTGCACCAAGGAGTA	CGTGGATGTGTTCATTGTTGA
Gli3	CACATTCCAATGAGAAACCG	ACAGTCTTCACGTGTTTCCG

Table 2. Sequence information of real-time qPCR primers

11. Western blot

Cell monolayer cultured in 60mm dish was prepared for protein sample. The culture medium was removed and the cells were washed with PBS 2 times. The cell monolayer was scrapped in 200 μl ice-cold RIPA buffer mixed with protease inhibitor cocktail (cOmplete™ Mini, Roche, US) on ice, transferred to a 1.5ml EP tube, and incubated for 10 minutes in ice. Protein samples from mouse tissue were homogenized by Precellys24 (Bertin Technologies, France) and ceramic beads with following settings; 5500 rpm, 30 seconds, 2 times. The cell and tissue lysates were centrifuged at 16000xG at 4℃, and the supernatant was transferred to a new 1.5ml EP tube.

The concentration of protein sample was determined by using Pierce BCA Protein Assay (Thermo Fisher Scientific, US) according to the manufacturer's protocol. Briefly, 2μl cell lysates and diluted albumin standard (BSA) were mixed with 200μl BCA reagent mixture (reagent A : reagent B = 49 : 1) and transferred to 96 well plate, and incubated at 37℃ for 30 minutes. The absorbance at 562nm was read using ELISA reader, and the protein concentration was interpolated from the standard curve.

The protein samples were subjected to electrophoresis on SDS-polyacrylamide gels. The gels were run with 70V for stacking gel and 120V for separating gel. After proper separation of protein ladder at the region of interest, the proteins were transferred to polyvinylidene fluoride (PVDF) membranes (Immobilon-P, Millipore, Billerica, MA, US) with 90V for 90 minutes. The membranes were blocked for 1 hour with 5 % skim milk in TBST (0.1% Tween-20 in TBS buffer), and incubated with primary antibody in 5% bovine serum albumin (BSA) overnight at 4℃ on a shaker. The membranes were washed with TBST 3 times, 10 minutes each, and incubated with secondary antibody in 5% skim milk in TBST for 1 hour at room temperature on a shaker. Again, the membranes were washed with TBST 3 times, 10 minutes each. The membranes were developed using ECL detection system (Amersham ECL PLUS Western blotting detection reagents, GE Healthcare Life Sciences, Buckinghamshire, UK) and CP-BU NEW x-ray film (AGFA HealthCare, Belgium). Following antibodies with indicated dilutions were used for immunoblot: anti-TULP4 (1:1000, described later in the Materials and Methods) followed by Anti-Rabbit IgG-peroxidase (1:5000, Sigma-Aldrich, US); anti-α-TUB (1:10000, DSHB, US) followed by Anti-Mouse IgG-peroxidase (1:10000, Sigma-

Aldrich, US); anti-β-ACTIN (1:2500, Stan-Cruz, US) followed by Anti-Goat IgG-peroxidase (1:10000).

12. Immunocytochemistry

The calvarial mouse osteoblasts were seeded on 18mm round cover glasses in 12 well plate. After 14 days of differentiation, the culture medium was removed, and the cells were washed with PBS 2 times and fixed with 4% paraformaldehyde in PBS for 10 minutes at room temperature. After washing with PBS 2 times, permeabilization was performed by 0.5% Triton X-100 in PBS for 3 minutes. After washing with PBS 2 times, the cells were blocked with 5% BSA in PBS for 1 hour. After washing with PBS 2 times, cover glass was removed from the plate, flipped, and transferred on a parafilm with primary antibody droplet (70μl). The cells were incubated overnight at 4℃. The cover glass was transferred back to 12 well plate and washed with PBS 2 times. Then, the cover glass was incubated on a secondary antibody droplet with ToPro3 (1:800, Invitrogen, US) in a same manner with primary antibody for 1 hour at room temperature in the dark. The cover glass was transferred back to

12 well plate, and washed with PBS 2 times, and air dried. The cover glass was mounted on a slide glass with VECTASHIELD mounting medium (Vector Lab, US). The primary antibodies were anti-TULP4 (1:50, described later in the Materials and Methods), anti-GLI2 (1:300)(Cho et al., 2008), and anti-GLI3 (1:50, Santa Cruz, US). The secondary antibodies were Alexa Fluor 488 Goat Anti-Rabbit IgG (Invitrogen, US) and Alexa Fluor 488 Goat Anti-Guinea Pig IgG (Invitrogen, US).

13. Generation of anti-TULP4 antibody

Glutathione S-transferase(GST)-tagged fusion protein of TULP4 (residue 1309~1547) was expressed in BL21 competent cells, and purified under denaturing condition. The fusion protein was injected into rabbit, and anti-TULP4 serum was collected and purified using PVDF membrane bound with the fusion protein.

14. Statistical analyses

Data were presented with mean ± standard deviation. Two-sample *t* tests were performed to compare two sets of data, and one-way ANOVA with post hoc Bonferroni tests were used in multiple sets of data. All statistical analyses were performed at a 5% significance level using SPSS for Windows, version 20.0 (SPSS, Chicago, IL, USA). Asterisks indicate the statistical significance.

Ⅲ. RESULTS

1. *Tulp4* is expressed in bone, and its expression is increased during early phase of osteoblastic differentiation.

Western blot was performed to examine the tissue distribution of TULP4 expression in mice. TULP4 was expressed ubiquitously, including brain, heart, liver, lung, testis, and skeletal muscle. These findings are in partial agreement with Li et al.(Li et al., 2001), which reported that *Tulp4* was mainly expressed in brain and testis in mice, while it was ubiquitously expressed in human demonstrated by northern blot (Figure 3A and B).

Next, *Tulp4* mRNA expression was examined in primary mouse calvarial osteoblast blasts, mouse bone (femur and tibia), and brain by real-time qPCR. *Tulp4* was expressed during differentiation of primary mouse calvarial osteoblasts, and it expression was increased until 7 days of differentiation and decreased thereafter. *Tulp4* mRNA was also expressed in bone and brain of mice, and the amount of expression was comparable to that in osteoblasts at 21 days of differentiation (Figure 3C).

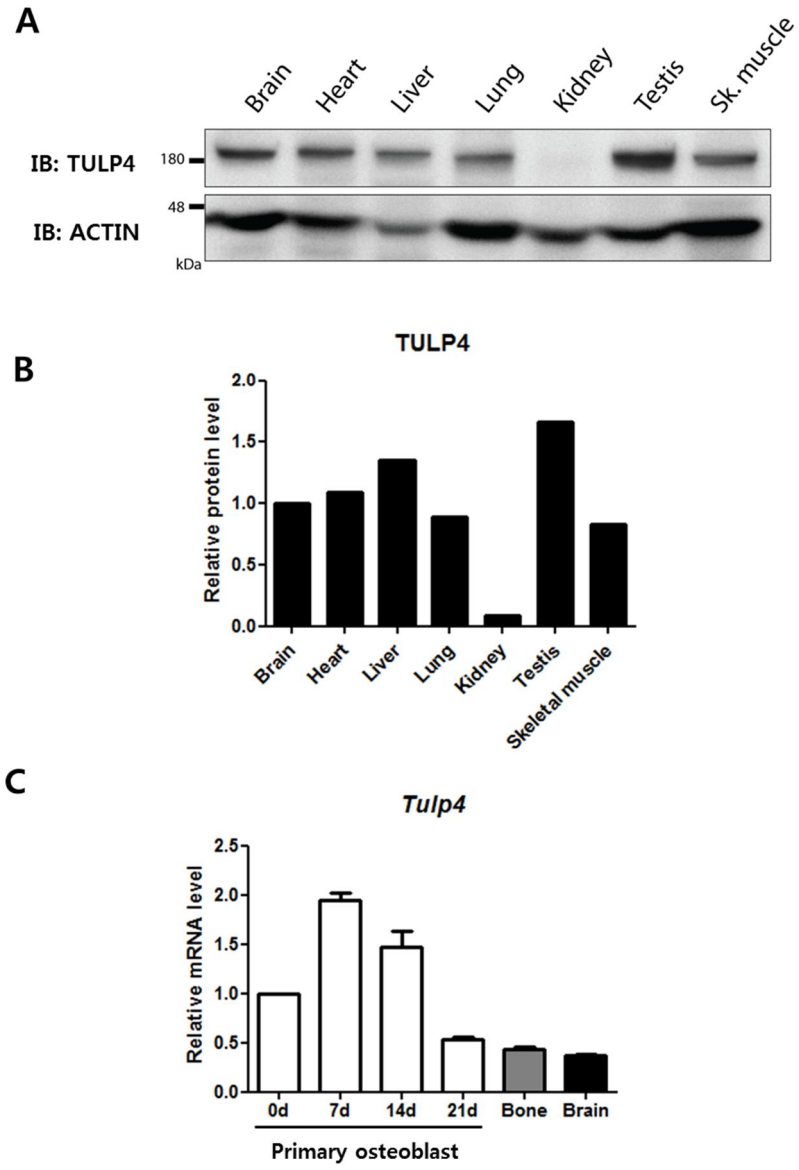

Figure 3. A. Tissue distribution of TULP4 protein expression in mice. B. Quantification of bands in A by using Image J software. C. *Tulp4* mRNA level determined by real-time qPCR.

2. Generation of *Tulp4* mutant mouse

Generation of *Tulp4* mutant mouse was confirmed by genomic PCR. Genomic PCR results of wild-type, tm1a, tm1c, and tm1d alleles were shown in Figure 4A. The genotype of *Tulp4* global knockout mouse was *Tulp4*(1d/1d) or *Tulp4*(-/-). The genotype of osteoblast-specific *Tulp4* knockout mouse was OC-Cre+; *Tulp4*(1c/1c), and its genomic PCR result was shown in Figure 4B.

To examine whether TULP4 knockout really occurred, TULP4 protein and *Tulp4* gene expression level were checked. No expression of TULP4 protein was observed in both brain and primary osteoblast lysates from *Tulp4*(-/-) genotype (Figure 4C). Also, *Tulp4* mRNA was not detected in osteoblast lysates (Figure 4D).

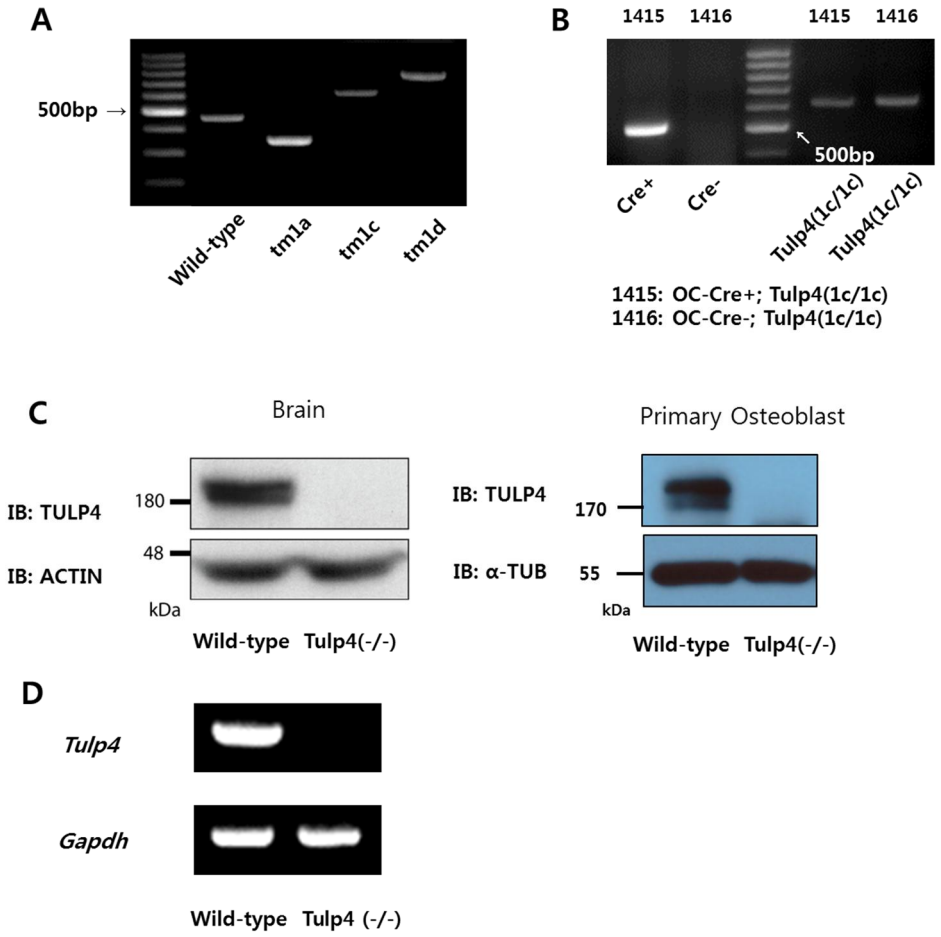

Figure 4. A. Genomic PCR for wild-type (466bp), tm1a (351bp), tm1c (620bp), and tm1d allele (720bp). B. Genomic PCR for #1415 mouse (OC-Cre+;Tulp4(1c/1c)) and #1416 mouse (OC-Cre-;Tulp4(1c/1c)). C. Western blots using anti-TULP4 antibody in brain and primary osteoblast lysates from wild-type and Tulp4(-/-). D. The results of RT-PCR from wild-type and Tulp4(-/-) osteoblasts.

3. *Tulp4* global knockout mice show neonatal lethality with no bone phenotype.

As mentioned above, *Tulp4* global knockout mice, either with *Tulp4*(1a/1a) or *Tulp4*(-/-) genotype, were lethal within 24 hours after birth. The cause of neonatal lethality was not clear, but *Tulp4*(-/-) neonates did not show the milk spot in the stomach, indicating abnormal feeding behavior in *Tulp4*(-/-) mice (Figure 5A).

To examine whether *Tulp4*(-/-) mice show any bone phenotype, alizarin red and alcian blue stainings were performed in neonates. *Tulp4*(-/-) mice did not show any difference in bone and cartilage development in neonates. No cleft palate was observed (Figure 5B and 5C).

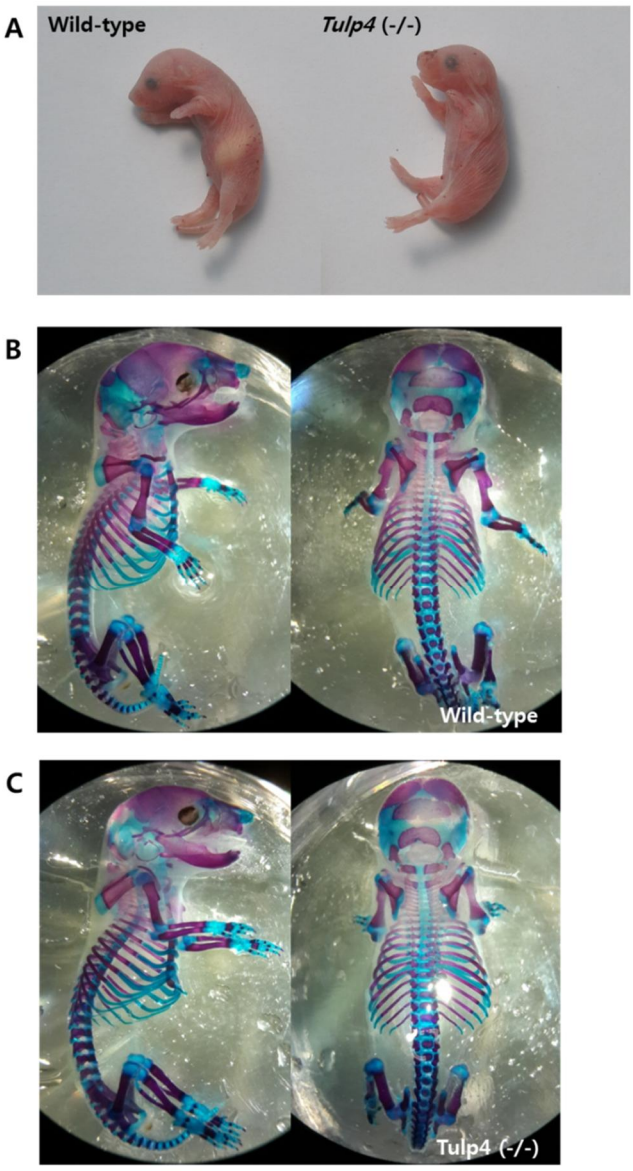

Figure 5. A. Wild-type and *Tulp4*(-/-) neonates. *Tulp4*(-/-) neonate did not show milk spot. B,C. Alizarin red (Red color) and alcian blue (Blue color) stainings in wild-type and *Tulp4*(-/-) littermates.

4. Osteoblast-specific *Tulp4* knockout adult mice show osteopetrotic phenotype.

To investigate the function of *Tulp4* in adult bone homeostasis, osteoblast-specific *Tulp4* knockout mice were generated using transgenic osteocalcin-cre and floxed *Tulp4* mice (*Tulp4* (1c/1c)).

Trabecular bone volume fraction and trabecular number were increased in 17-week-old male mature osteoblast-specific Tulp4 knockout mice (OC-Cre+ ; *Tulp4*(1c/1c)), compared to littermate wild-type mice (*Tulp4*(1c/1c)). Trabecular thickness and separation were not changed in osteoblast-specific *Tulp4* knockout mice (Figure 6A and B). Increased bone mass in osteoblast-specific *Tulp4* knockout mice were also found in histological section stained with H & E (Figure 7A). Histomorphometric analysis showed that the number of osteoblasts was increased in osteoblast-specific *Tulp4* knockout mice (Figure 7B). These results demonstrated that *Tulp4* negatively regulates bone homeostasis *in vivo*.

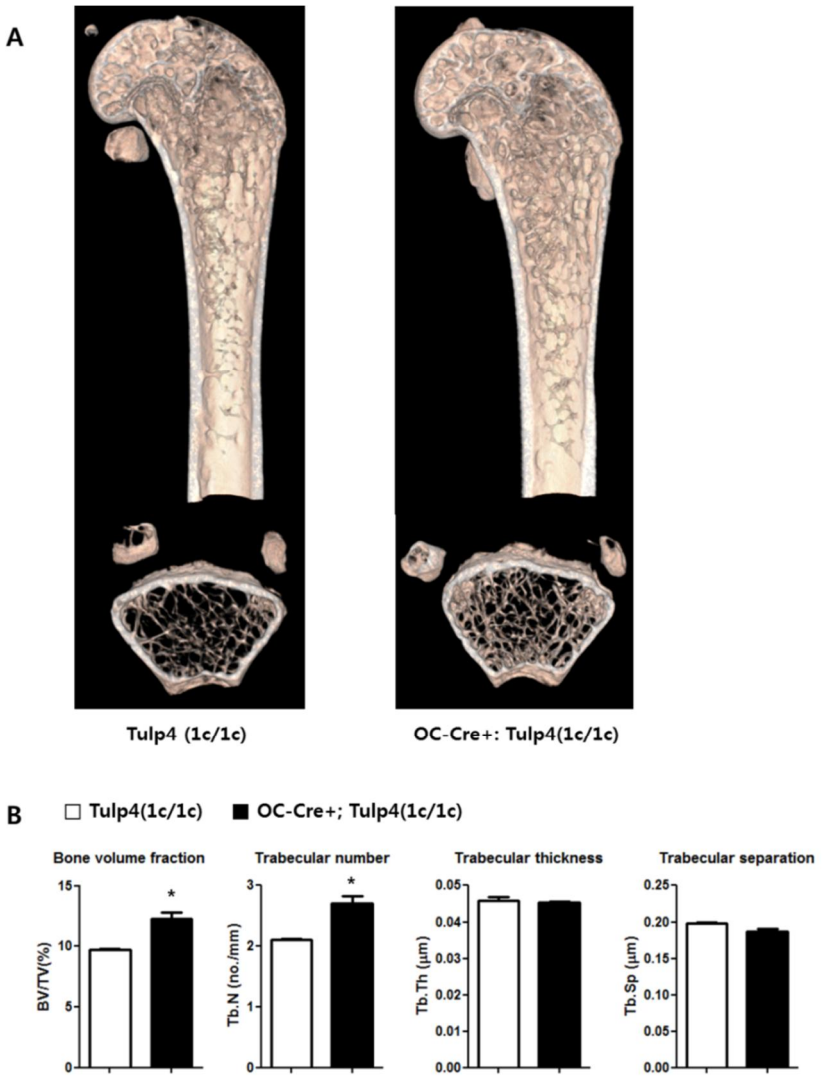

Figure 6. A. Representative image of sagittal and transverse sections of wild-type and osteoblast-specific *Tulp4* knockout male littermates (17-week-old). B. Morphometric measurements of CT images (n = 2), analyzed by two-sample t test. $*P < 0.05$.

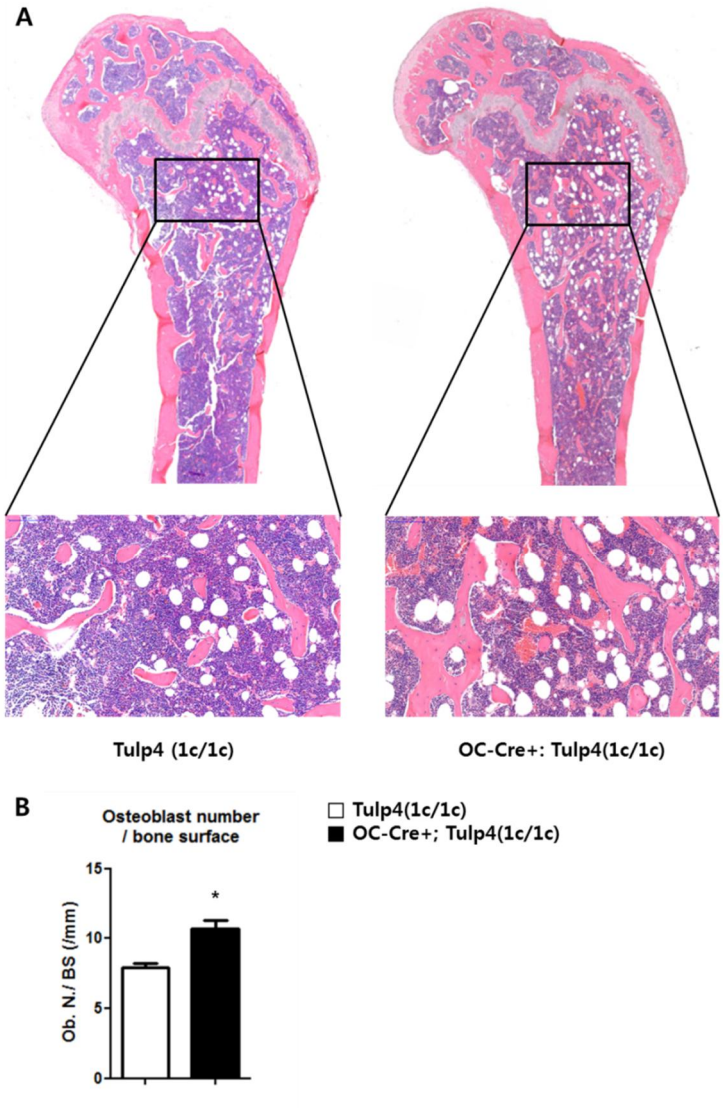

Figure 7. A. Representative histological images stained with H&E of wild-type and osteoblast-specific *Tulp4* knockout male littermates (17-week-old). B. Morphometric measurements of osteoblast numbers per bone surface (n = 2), analyzed by two-sample t test. $*P < 0.05$.

5. *Tulp4* inhibits osteoblastic differentiation in a cell-autonomous manner.

To investigate whether negative regulation of *Tulp4* in bone homeostasis was in a cell-autonomous manner, primary mouse calvarial cells were isolated and differentiation was induced. ALP staining after 7 days of differentiation demonstrated that ALP activity was enhanced in *Tulp4*(-/-) osteoblasts (Figure 8A and C). Also, mineralized nodules were increased in *Tulp4*(-/-) osteoblasts in alizarin red S staining after 21 days of differentiation (Figure 8B and D).

Expression levels of osteoblast marker genes were also markedly higher in *Tulp4*(-/-) cells from early phase of differentiation until late phase of differentiation. *Sp7* (osterix), *Bglap* (osteocalcin), *Ibsp* (bone sialoprotein) were nearly 2-fold, 6-fold, and 4-fold increased in *Tulp4* (-/-) cells in 7 days of differentiation, respectively. These changes were more profound in 21 days of differentiation (Figure 9A and B). These results demonstrated that *Tulp4* inhibits osteoblastic differentiation from early phase to late phase of differentiation in a cell-autonomous manner.

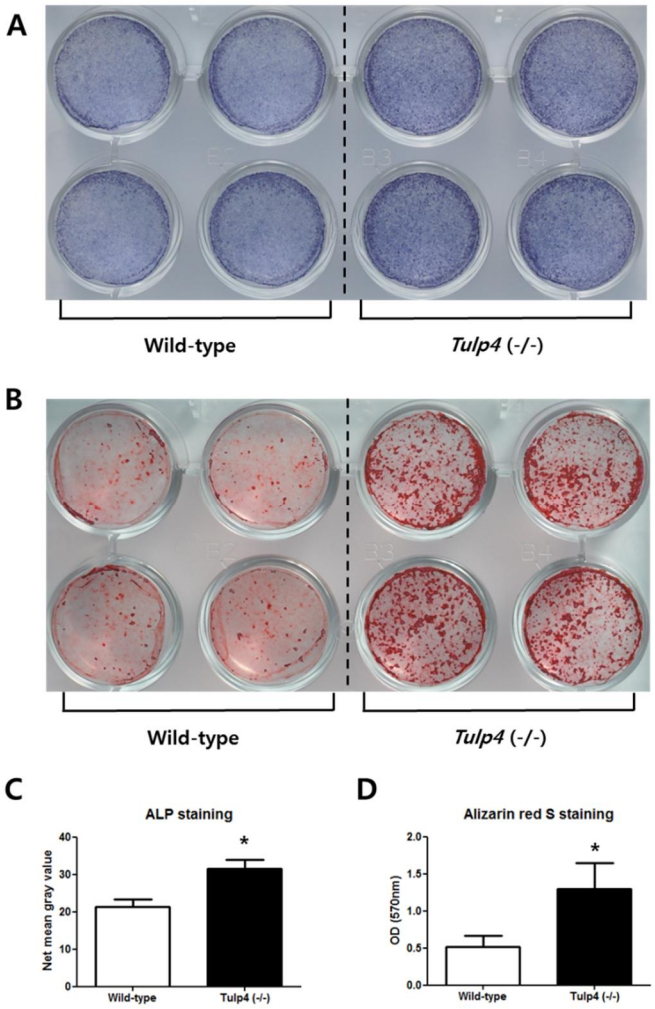

Figure 8. A. ALP staining after 7 days of differentiation. B. Alzarin red S staining after 21 days of differentiation. C. Quantification of ALP staining by using ImageJ software (n = 2), analyzed by two-sample t test. $*P < 0.05$. D. Quantification of alizarin red S staining by CPC extraction method (n = 3), analyzed by two-sample t test. $*P < 0.05$.

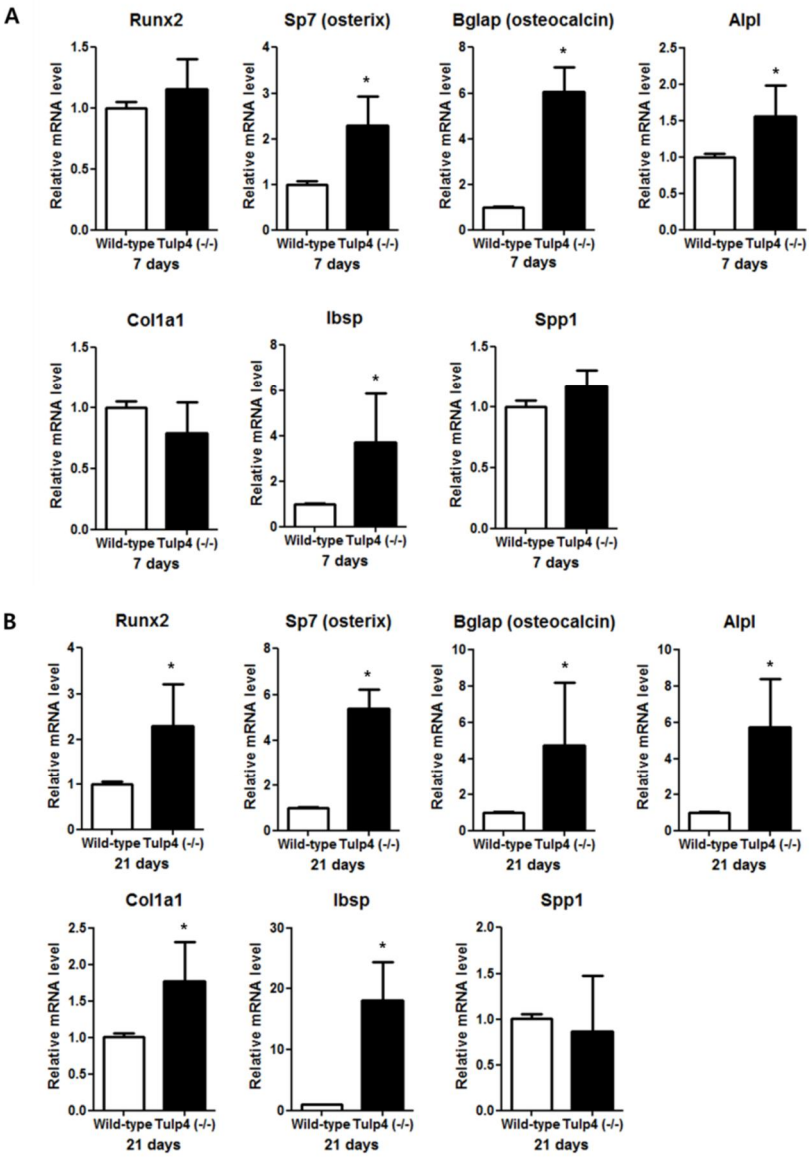

Figure 9. Real-time qPCR results of osteoblast marker genes in early phase (7 days, A) and late phase (21 days, B) of differentiation (n = 3), analyzed by two-sample t test. $*P < 0.05$.

6. Hedgehog signaling was enhanced in *Tulp4* knockout osteoblasts.

There are several major pathways that have been known to regulate osteoblastic differentiation: hedgehog signaling, notch singaling, WNT signaling, BMP signaling, and FGF singaling pathways (Long, 2012). Since *Tulp3*, another member of Tubby family, has been known to negatively regulate hedgehog signaling via ciliary trafficking of GPR161 (Mukhopadhyay et al., 2013), hedgehog signaling in *Tulp4*(-/-) cells was firstly investigated.

Surprisingly, expressions of *Ptch1* and *Gli1*, which are the direct readout of hedgehog signaling, were higher in *Tulp4*(-/-) osteoblasts than in wild-type osteoblasts, and these differences were greater in late phase of differentiation than early phase of differentiation. *Gli2* and *Gli3* expressions were not changed, although *Gli2* expression in 21 days of differentiation was slightly decreased in *Tulp4*(-/-) osteoblasts (Figure 10).

Next, localizations of GLI2 and GLI3 were investigated by immunocytochemistry, since previous studies reported that sonic hedgehog or SAG (Smo agonist) induce accumulation of GLI2 and GLI3 full

length in nucleus (Humke et al., 2010; Kim et al., 2009). Indeed, GLI2 full length and GLI3 were markedly accumulated in nucleus of osteoblast at 14 days of differentiation, although anti-GLI3 antibody could not differentiate the full length or repressor form of GLI3 (Figure 11).

Collectively, these findings demonstrated that *Tulp4* negatively regulates hedgehog signaling during osteoblastic differentiation.

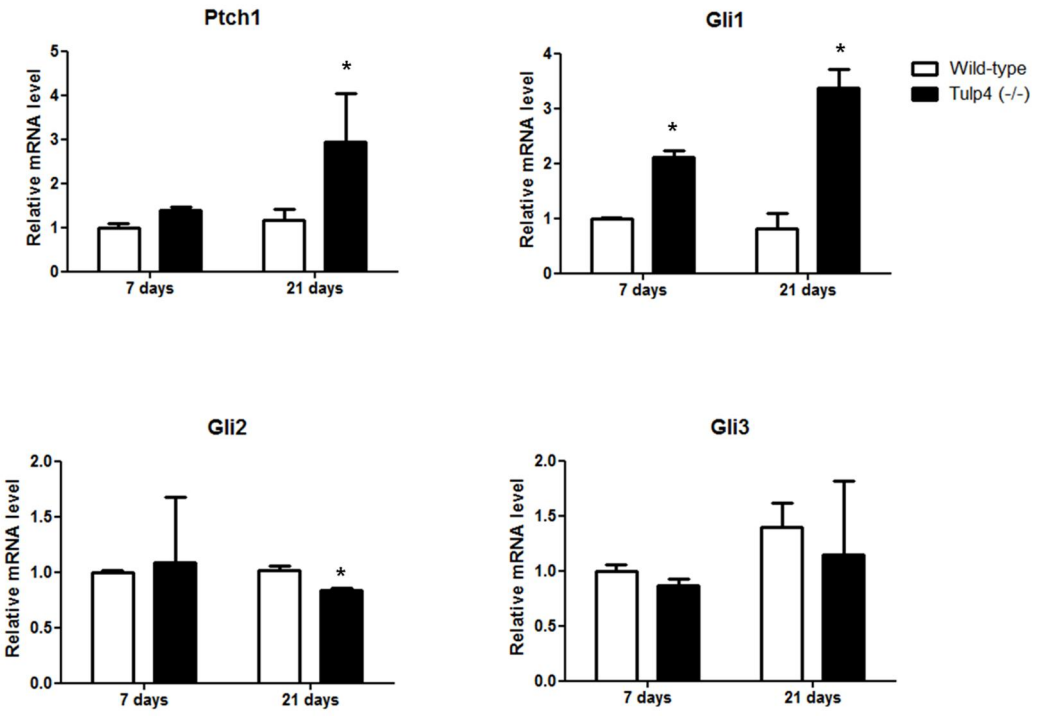

Figure 10. Real-time qPCR results of hedgehog signaling genes in 7 days and 21 days of differentiation (n = 3), analyzed by two-sample t test. $*P < 0.05$.

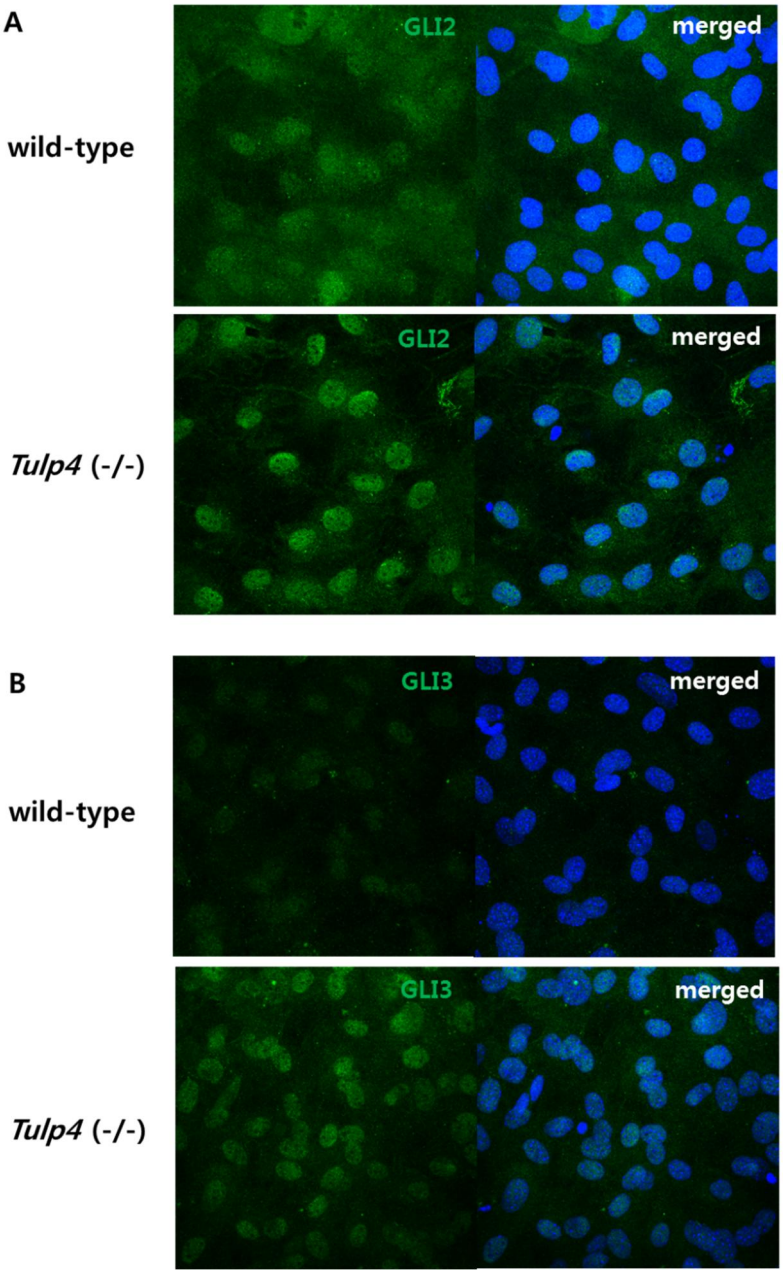

Figure 11. Immunocytochemistry results of primary osteoblasts at 14 days of differentiation. A. GLI2. B. GLI3. DNA was stained by To-pro3.

7. Increased expression of *Ihh* was the cause of increased hedgehog signaling in *Tulp4* knockout osteoblasts.

Hedgehog signaling is initiated by binding of hedgehog ligand to PTCH1 receptor in primary cilia. Thus, expressions of *Ihh* and *Shh* were investigated. Surprisingly, expression of *Ihh* was increased in *Tulp4*(-/-) osteoblasts compared to wild-type, and it was pronounced in 21 days of differentiation as with *Gli1* expression. Expression of *Shh* was not changed, indicating that the inhibition effect of *Tulp4* in transcription of *Ihh* was specific (Figure 12).

Next, to examine whether the increased *Ihh* expression was the sole cause of the increased hedgehog signaling in *Tulp4* knockout osteoblasts, 5E1 (hedgehog neutralizing antibody) and cyclopamine (Smo antagonist) were treated during differentiation of primary osteoblast. Treatment of 5E1 decreased the endogenous hedgehog signaling from the concentration of 10μg/ml in a dose dependent manner, indicating that 5E1 was effectively working at indicated concentrations. The concentration of 2μg/ml did not affect the endogenous hedgehog signaling. Surprisingly, increased *Gli1* expression in *Tulp4*(-/-) cells treated with non-specific

antibody (control) was blocked at 2μg/ml 5E1 treatment. The hedgehog phenotype was also abolished by the treatment of 2μM cyclopamine, confirming that the cause of increased hedgehog signaling occurred before the SMO recruitment to primary cilia (Figure 13). These findings demonstrated that increased expression of *Ihh* was the sole cause of the increase hedgehog signaling in *Tulp4*(-/-) osteoblasts.

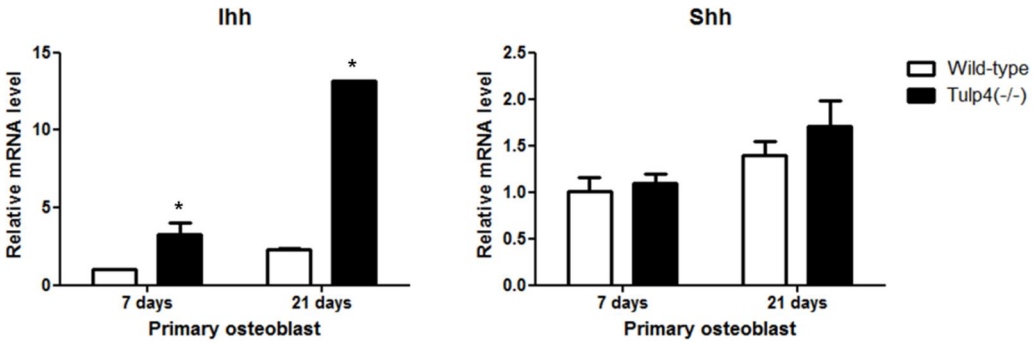

Figure 12. Real-time qPCR results of *Ihh* and *Shh* in primary osteoblast during differentiation, (n = 2), analyzed by two-sample t test. $*P < 0.05$.

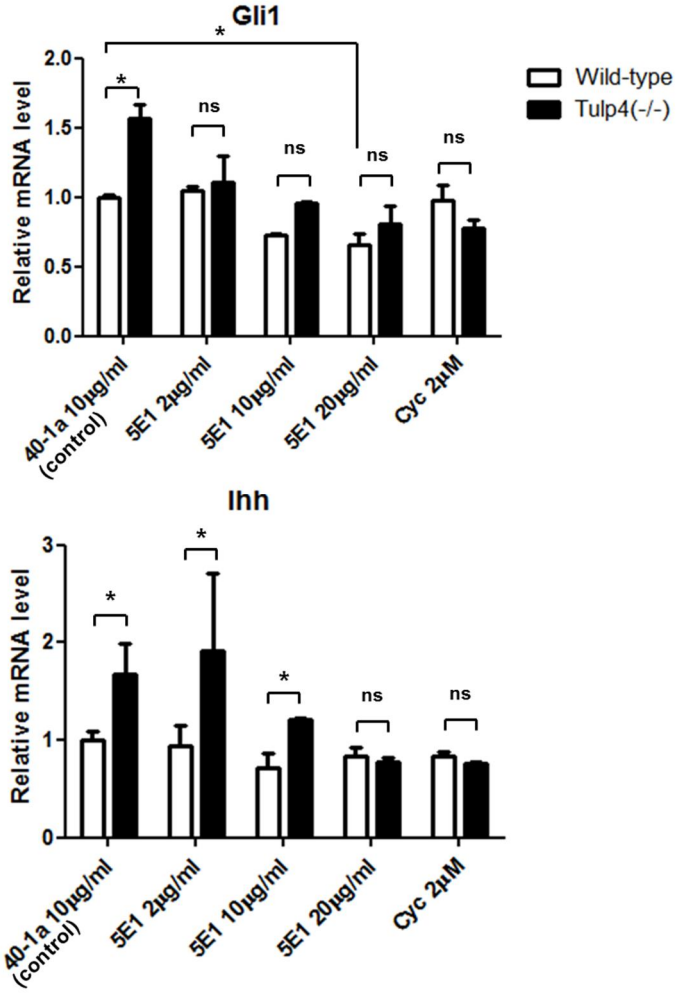

Figure 13. Real-time qPCR results of *Gli1* and *Ihh* in wild-type and *Tulp4*(-/-) osteoblasts treated with or without 5E1 antibody and cyclopamine after 7 days of differentiation, (n = 2), analyzed by two-sample t test and one-way ANOVA and post hoc Bonferroni test. $*P < 0.05$. ns: non-significant.

8. TULP4 is localized to nucleus in primary osteoblast.

To further investigate the mechanism of *Tulp4* in regulation of hedgehog signaling, localization of TULP4 was examined using immunofluorescence imaging and cell fractionation followed by western blot in the primary osteoblast.

TULP4 was observed in nucleus as nuclear dots by immunofluorescence imaging (Figure 14). This finding is in contrast with previous study that GFP-tagged full length of TULP4 was localized exclusively to cytosol in HEK293 cells, although GFP-tagged C-terminal TULP4 was observed as nuclear dots (Li et al., 2001). Nuclear localization of TULP4 was also confirmed by western blot, in which TULP4 was observed in the nuclear fraction. Cytosolic localization of TULP4 was not clear due to the significant contamination of nuclear marker (Histone-H3) in the cytosolic fraction (Figure 15).

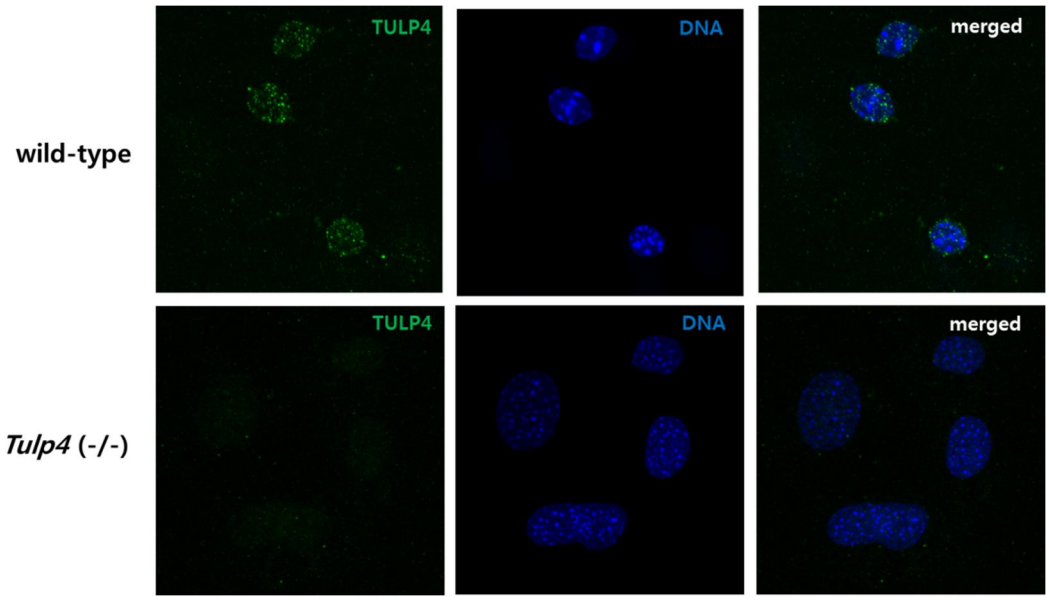

Figure 14. Immunocytochemistry results for localization of TULP4 in primary osteoblast after 14 days of differentiation.

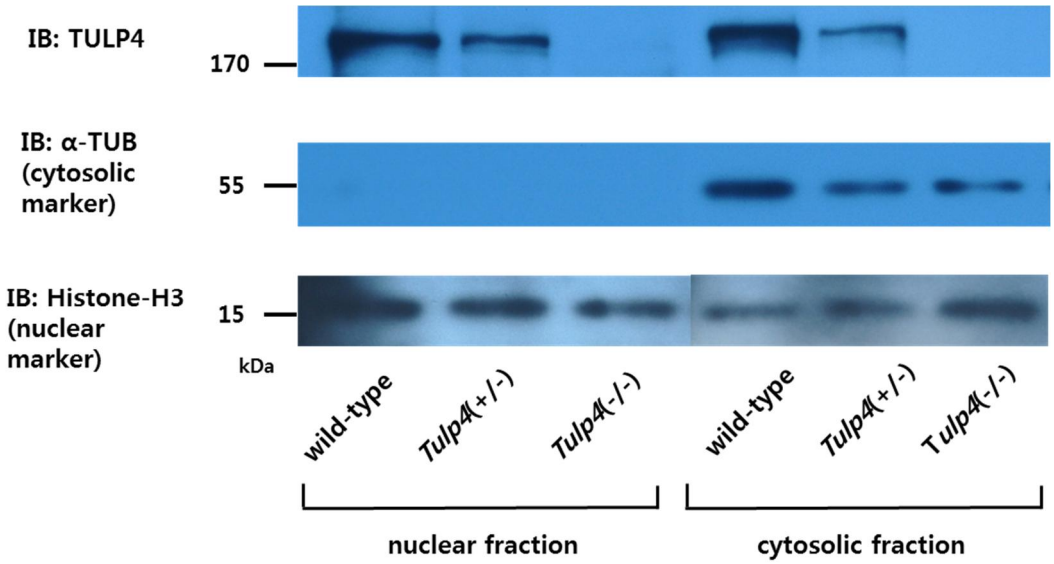

Figure 15. Western blots following subcellular fractionation of wild-type, *Tulp4*(+/−), and *Tulp4*(−/−) osteoblasts

Ⅳ. DISCUSSION

In this study, we generated osteoblast-specific *Tulp4* knockout mice, and osteoblastic differentiation was also investigated *in vitro* by using primary mouse calvarial osteoblasts. We identified novel functions of *Tulp4* that inhibits bone formation and negatively regulates hedgehog signaling by inhibition of *Ihh* expression. However, several questions still remain regarding the function of *Tulp4*.

The mechanism of how *Tulp4* inhibits the expression of *Ihh* should be further investigated. We demonstrated that TULP4 was localized in nucleus in primary osteoblasts during differentiation. This finding suggests a possibility that TULP4 may be a transcriptional repressor for *Ihh*. This possibility is supported by the fact that the tubby domain can bind to DNA (Ikeda et al., 2002).

Another more convincing hypothesis is that TULP4 may regulate the ubiquitination of unknown transcription factor for *Ihh* expression. High throughput affinity capture mass spectrometric analysis revealed that TULP4 is a binding partner for Cullin 5, a scaffold of E3 Cullin-RING ubiquitin ligase(Bennett et al., 2010). Also, TULP4 has structural similarity

with other proteins belonging to the E3 ligase and determining substrate specificity, such as SOCS domain, which can interact with Elonging BC complex, and WD40 repeat domain, which determines substrate specificity. In this regard, it has been suggested that TULP4 may participate in ubiquitination process, but the target protein is still unknown. From the results of this study, the unknown target protein is likely a transcription factor for *Ihh* expression. Well-known transcription factors for *Ihh* expression from the literature search are RUNX2(Yoshida et al., 2004), SMAD 1 & 5 (Retting et al., 2009), SMAD4(Seki and Hata, 2004), ATF4(Wang et al., 2009), C/EBPβ(Ushijima et al., 2014), CBFβ(Wu et al., 2014), THRβ(Xing et al., 2016), and VEGFA(Duan et al., 2015). Immunoprecipitation with anti-TULP4 antibody followed by LC-MS/MS may reveal a target protein of TULP4 in ubiquitination.

Second, it is still not known why *Tulp4*(-/-) mice show neonatal lethality. While global *Tulp4* knockout mice were lethal within 24 hours after birth, osteoblast-specific *Tulp4* knockout mice showed normal growth. However, neural progenitor-specific *Tulp4* knockout mice using transgenic Nestin-Cre mice recapitulated the neonatal lethality phenotype (data not shown). This indicates that *Tulp4* also plays a critical role in

neural tissue. Considering that *Tulp4* knockout neonates show abnormal feeding behavior and it may come from the neural defect, the cause of lethality may be neuromuscular defects, such as olfaction, sensory-motor, and hypothalamus problem (Turgeon and Meloche, 2009).

Lastly, osteoblast-specific *Tulp4* knockout mice showed osteopetrotic phenotype, which seems to contradict the reports of human association studies. Previous studies reported that SNP in 3'UTR of *TULP4* was associated with short stature (Lango Allen et al., 2010), and genetic variants in *TULP4* gene was associated with cleft lip with or without cleft palate (Vieira et al., 2015). One possibility is that those genetic variants may increase the expression of *TULP4*, rather than decrease it, leading to the osteopenic phenotype. Future studies may include human sample and investigate whether those genetic variants affect the expression of *TULP4*.

The novel finding that *Tulp4* negatively regulates bone formation has medical significance, since TULP4 can be a therapeutic target for osteoporosis treatment. The fact that osteoblast-specific *Tulp4* knockout mice showed osteopetrotic phenotype in adults, not in neonates, indicates that *Tulp4* plays a critical role in adult bone homeostasis. This makes

TULP4 a good candidate for therapeutic target in age-related osteoporosis. Screening for selective inhibitor of TULP4 function may lead to the development of a new drug for treating osteoporosis.

Ⅴ. CONCLUSION

This study was aimed to investigate possible roles of *TULP4* in bone homeostasis using osteoblast-specific *Tulp4* knockout mouse model and *in vitro* primary mouse calvarial cell culture system.

1. Bone mass was increased in osteoblast-specific *Tulp4* knockout mice.

2. *Tulp4* inhibited osteoblastic differentiation in a cell autonomous manner *in vitro*.

3. *Tulp4* negatively regulated hedgehog signaling in osteoblast cell lineage by inhibition of *Ihh* expression.

4. TULP4 was localized to nucleus in the primary osteoblast.

Ⅵ. REFERENCES

Bennett EJ, Rush J, Gygi SP, Harper JW: Dynamics of cullin-RING ubiquitin ligase network revealed by systematic quantitative proteomics. *Cell* 143(6): 951-965, 2010.

Burge R, Dawson-Hughes B, Solomon DH, Wong JB, King A, Tosteson A: Incidence and economic burden of osteoporosis-related fractures in the United States, 2005-2025. *J Bone Miner Res* 22(3): 465-475, 2007.

Cho A, Ko HW, Eggenschwiler JT: FKBP8 cell-autonomously controls neural tube patterning through a Gli2- and Kif3a-dependent mechanism. *Dev Biol* 321(1): 27-39, 2008.

Cosman F, de Beur SJ, LeBoff MS, Lewiecki EM, Tanner B, Randall S, et al.: Clinician's Guide to Prevention and Treatment of Osteoporosis. *Osteoporos Int* 25(10): 2359-2381, 2014.

Duan X, Murata Y, Liu Y, Nicolae C, Olsen BR, Berendsen AD: Vegfa regulates perichondrial vascularity and osteoblast differentiation in bone development. *Development* 142(11): 1984-1991, 2015.

Humke EW, Dorn KV, Milenkovic L, Scott MP, Rohatgi R: The output of Hedgehog signaling is controlled by the dynamic association between Suppressor of Fused and the Gli proteins. *Genes Dev* 24(7): 670-682, 2010.

Ikeda A, Ikeda S, Gridley T, Nishina PM, Naggert JK: Neural tube defects and neuroepithelial cell death in Tulp3 knockout mice. *Hum Mol Genet* 10(12): 1325-1334, 2001.

Ikeda A, Nishina PM, Naggert JK: The tubby-like proteins, a family with roles in neuronal development and function. *J Cell Sci* 115(Pt 1): 9-14, 2002.

Kim J, Kato M, Beachy PA: Gli2 trafficking links Hedgehog-dependent activation of Smoothened in the primary cilium to transcriptional activation in the

nucleus. *Proc Natl Acad Sci U S A* 106(51): 21666-21671, 2009.

Kumar V, Sinha RK: Bisphosphonate Related Osteonecrosis of the Jaw: An Update. *J Maxillofac Oral Surg* 13(4): 386-393, 2014.

Lango Allen H, Estrada K, Lettre G, Berndt SI, Weedon MN, Rivadeneira F, et al.: Hundreds of variants clustered in genomic loci and biological pathways affect human height. *Nature* 467(7317): 832-838, 2010.

Li QZ, Wang CY, Shi JD, Ruan QG, Eckenrode S, Davoodi-Semiromi A, et al.: Molecular cloning and characterization of the mouse and human TUSP gene, a novel member of the tubby superfamily. *Gene* 273(2): 275-284, 2001.

Lin AE, Traum AZ, Sahai I, Keppler-Noreuil K, Kukolich MK, Adam MP, et al.: Sensenbrenner syndrome (Cranioectodermal dysplasia): clinical and molecular analyses of 39 patients including two new patients. *Am J Med Genet A* 161A(11): 2762-2776, 2013.

Long F: Building strong bones: molecular regulation of the osteoblast lineage. *Nat Rev Mol Cell Biol* 13(1): 27-38, 2012.

Mukhopadhyay S, Wen X, Chih B, Nelson CD, Lane WS, Scales SJ, et al.: TULP3 bridges the IFT-A complex and membrane phosphoinositides to promote trafficking of G protein-coupled receptors into primary cilia. *Genes Dev* 24(19): 2180-2193, 2010.

Mukhopadhyay S, Wen X, Ratti N, Loktev A, Rangell L, Scales SJ, et al.: The ciliary G-protein-coupled receptor Gpr161 negatively regulates the Sonic hedgehog pathway via cAMP signaling. *Cell* 152(1-2): 210-223, 2013.

Phan TC, Xu J, Zheng MH: Interaction between osteoblast and osteoclast: impact in bone disease. *Histol Histopathol* 19(4): 1325-1344, 2004.

Retting KN, Song B, Yoon BS, Lyons KM: BMP canonical Smad signaling through Smad1 and Smad5 is required for endochondral bone formation. *Development* 136(7): 1093-1104, 2009.

Seki K, Hata A: Indian hedgehog gene is a target of the bone morphogenetic

protein signaling pathway. *J Biol Chem* 279(18): 18544-18549, 2004.

Turgeon B, Meloche S: Interpreting neonatal lethal phenotypes in mouse mutants: insights into gene function and human diseases. *Physiol Rev* 89(1): 1-26, 2009.

Ushijima T, Okazaki K, Tsushima H, Ishihara K, Doi T, Iwamoto Y: CCAAT/enhancer binding protein beta regulates expression of Indian hedgehog during chondrocytes differentiation. *PLoS One* 9(8): e104547, 2014.

Vahle JL, Sato M, Long GG, Young JK, Francis PC, Engelhardt JA, et al.: Skeletal changes in rats given daily subcutaneous injections of recombinant human parathyroid hormone (1-34) for 2 years and relevance to human safety. *Toxicol Pathol* 30(3): 312-321, 2002.

Vieira AR, de Carvalho FM, Johnson L, DeVos L, Swailes AL, Weber ML, et al.: Fine Mapping of 6q23.1 Identifies TULP4 as Contributing to Clefts. *Cleft Palate Craniofac J* 52(2): 128-134, 2015.

Wang W, Lian N, Li L, Moss HE, Wang W, Perrien DS, et al.: Atf4 regulates chondrocyte proliferation and differentiation during endochondral ossification by activating Ihh transcription. *Development* 136(24): 4143-4153, 2009.

Wu M, Li YP, Zhu G, Lu Y, Wang Y, Jules J, et al.: Chondrocyte-specific knockout of Cbfbeta reveals the indispensable function of Cbfbeta in chondrocyte maturation, growth plate development and trabecular bone formation in mice. *Int J Biol Sci* 10(8): 861-872, 2014.

Xing W, Aghajanian P, Goodluck H, Kesavan C, Cheng S, Pourteymoor S, et al.: Thyroid hormone receptor-beta1 signaling is critically involved in regulating secondary ossification via promoting transcription of the Ihh gene in the epiphysis. *Am J Physiol Endocrinol Metab* 310(10): E846-854, 2016.

Yoshida CA, Yamamoto H, Fujita T, Furuichi T, Ito K, Inoue K, et al.: Runx2 and Runx3 are essential for chondrocyte maturation, and Runx2 regulates limb growth through induction of Indian hedgehog. *Genes Dev* 18(8): 952-963, 2004.

국문요약

조골 세포에서 Tubby-like protein 4 에 의한 hedgehog 신호 전달 경로의 조절

(지도교수 백 형 선)

연세대학교 대학원 치의학과

김 성 진

Tubby-like protein 4 (TULP4)는 Tubby superfamily의 구성원으로서, 뼈의 항상성과 관련된 기능을 할 것으로 추측되고 있으나, 현재까지 그 기능에 대해 알려진 바가 없다. 따라서 본 연구에서는 Cre-lox 시스템을 이용하여 조골세포 특이적으로 *Tulp4*를 knockout 시킨 마우스를 제작하고, 일차 조골세포 배양을 통해 뼈의 항상성과 관련한 *Tulp4*의 기능을 조사하였다.

*Tulp4*는 뼈에서 높은 수준으로 발현되고 있으며, 조골세포의 분화 초기에 발현량이 증가하였다. 모든 조직에서 *Tulp4*를 knockout시킨 마우스는 출생 후 24시간 내에 사망하였고 뼈에 이상 소견을 보이지 않았으나, 조골세포

특이적으로 *Tulp4*를 knockout 시킨 마우스의 성체에서는 골밀도가 증가하는 양상이 관찰되었다. 또한 *Tulp4*가 knockout된 일차 조골세포에서 분화가 증가함이 관찰되어, *Tulp4*가 cell-autonomous하게 조골세포의 분화를 억제함을 알 수 있었다. 이후 조골세포의 분화와 관련된 신호전달경로를 살펴본 결과, *Tulp4* knockout 조골세포에서 *Ptch1*과 *Gli1* mRNA의 발현이 증가되어 있었고, 이는 hedgehog signaling이 증가되어 있음을 나타냈다. 또한 *Tulp4* knockout 조골세포에서 *Ihh*의 발현이 증가하여 있었고, hedgehog neutralizing 항체인 5E1에 의해 증가했던 *Gli1* mRNA 레벨이 wild-type 수준으로 떨어짐을 확인함으로서 *Ihh*의 발현 증가가 hedgehog signaling의 증가 원인임을 알 수 있었다.

본 연구에서는 과거 기능이 알려지지 않았던 *Tulp4*가 뼈의 항상성 조절에 중요한 역할을 함을 밝혔다. *Tulp4*는 *Ihh*의 발현 억제를 통하여 hedgehog signaling을 음성 조절하였고, 조골세포의 분화 억제를 통해 골형성을 억제하였다.

핵심 되는 말: Tubby-like protein 4, 뼈, 조골세포 분화, hedgehog